Synaptosomal Actin Dynamics in the Developmental Visual Cortex Regulate Behavioral Visual Acuity in Rats

Ai-Ling Bi,[1–3] Yue-Ying Zhang,[1,3,4] Zhi-Yuan Lu,[1,3] Hong-Ying Tang,[1,3,5] Xiu-Yan Zhang,[1,3,5] Zi-Han Zhang,[1,3,5] Bo-Qin Li,[6] Da-Dong Guo,[1–3] Sheng Gong,[1,3] Qian Li,[1,3] Xing-Rong Wang,[1,3,5] Xiu-Zhen Lu,[1,3,5] and Hong-Sheng Bi[1–3,5]

[1]Shandong Provincial Key Laboratory of Integrated Traditional Chinese and Western Medicine for Prevention and Therapy of Ocular Diseases, Key Laboratory of Integrated Traditional Chinese and Western Medicine for Prevention and Therapy of Ocular Diseases in Universities of Shandong, Jinan, Shandong Province, China
[2]Eye Institute of the Shandong University of Traditional Chinese Medicine, Jinan, Shandong Province, China
[3]Shandong University of Traditional Chinese Medicine, Jinan, Shandong Province, China
[4]School of Basic Medical Sciences, Shandong First Medical University, Jinan, Shandong Province, China
[5]Affiliated Eye Hospital of Shandong University of Traditional Chinese Medicine, Jinan, Shandong Province, China
[6]Ultrastructural Laboratory, Shandong WEI-YA Biotech Company, Jinan, Shandong Province, China

Correspondence: Hong-Sheng Bi, Affiliated Eye Hospital of Shandong University of Traditional Chinese Medicine, No. 48 Ying-xiong-shan Road, Jinan 250002, Shandong, China;
hongshengbi1@163.com.

A-LB, Y-YZ, and Z-YL contributed equally to this work.

Received: July 28, 2020
Accepted: May 15, 2021
Published: June 17, 2021

Citation: Bi A-L, Zhang Y-Y, Lu Z-Y, et al. Synaptosomal actin dynamics in the developmental visual cortex regulate behavioral visual acuity in rats. *Invest Ophthalmol Vis Sci.* 2021;62(7):20.
https://doi.org/10.1167/iovs.62.7.20

Purpose. Synaptosomal actin dynamics are essential for synaptic structural stability. Whether actin dynamics are involved in structural and functional synaptic plasticity within the primary visual cortex (V1) or behavioral visual acuity in rats has still not been thoroughly investigated.

Methods. Synaptosome preparation and western blot analysis were used to analyze synaptosomal actin dynamics. Transmission electron microscopy was used to detect synaptic density and mitochondrial area alterations. A visual water maze task was applied to assess behavioral visual acuity. Microinjection of the actin polymerization inhibitor or stabilizer detected the effect of actin dynamics on visual function.

Results. Actin dynamics, the mitochondrial area, and synaptic density within the area of V1 are increased during the critical period for the development of binocularity. Microinjection of the actin polymerization inhibitor cytochalasin D into the V1 decreased the mitochondrial area, synaptic density, and behavioral visual acuity. Long-term monocular deprivation reduced actin dynamics, the mitochondrial area, and synaptic density within the V1 contralateral to the deprived eye compared with those ipsilateral to the deprived eye and impaired visual acuity in the amblyopic eye. In addition, the mitochondrial area, synaptic density, and behavioral visual acuity were improved by stabilization of actin polymerization by jasplakinolide microinjection.

Conclusions. During the critical period of visual development of binocularity, synaptosomal actin dynamics regulate synaptic structure and function and play roles in behavioral visual acuity in rats.

Keywords: actin dynamics, mitochondrion, synapse, visual cortex, visual development

Actin, a major cytoskeletal protein in the pre- and postsynaptic terminals, plays a key role in synaptic plasticity by the modulation of its two states, the spherical actin monomer (G-actin) and filamentous actin polymer (F-actin).[1–4] Actin dynamics-related cortical plasticity has long been investigated in connection with learning and memory processes.[5–9] Neural development and the processes of learning and memory share similar molecular and cellular mechanisms. Synaptic density and actin cytoskeletal dynamics within the visual cortex have been reported to increase during a critical period of visual development.[10,11] However, during the critical period for the development of binocularity, the roles of actin dynamics in regulating synaptic structure and function and behavioral visual acuity in rats remain unclear.

Amblyopia is a disease occurring in infancy and childhood related to ocular dominance plasticity and visual development. Numerous studies have shown that neurotransmitters and receptors, such as the *N*-methyl-D-aspartate (NMDA)-type glutamate receptor, gamma-amino butyric acid (GABA), and neurotrophins, among others, are involved in ocular dominance plasticity.[12–14] Actin is also a downstream molecule of glutamate, GABA, and neuronal growth factors, which play essential roles during ocular dominance plasticity.[13,15–17]

In the present study, we hypothesized that synaptosomal actin dynamics also contribute to the process of visual development and the pathogenesis of amblyopia. We addressed the question of whether or not synaptosomal actin dynamics regulate structural and functional synaptic plasticity

during postnatal visual development. Moreover, the roles of actin dynamics in behavioral visual acuity were investigated. Furthermore, using the classic monocular deprivation (MD) procedure, we investigated whether or not actin dynamics correlated with changes in visual acuity during the critical period for the development of binocularity.

Materials and Methods

Subjects

Sprague Dawley (SD) rats of either sex (13 to 45 days old) were used throughout all experiments. All animals were maintained in an environment with a temperature of 22 ± 2°C and on a half-day light/dark period with free access to food and water. All protocols were consistent with the National Institutes of Health Guide for the Care and Use of Laboratory Animals. All experiments were permitted by the Institutional Animal Ethics Committee of the Eye Institute of the Shandong University of Traditional Chinese Medicine.

Reagents

Cytochalasin D (125 ng/µL in normal saline and 1% dimethylsulfoxide [DMSO]), anti-glyceraldehyde 3-phosphate dehydrogenase (GAPDH), and anti-actin were purchased from Sigma-Aldrich (St. Louis, MO, USA). Jasplakinolide (20 ng/µL in normal saline containing 2% DMSO) was obtained from Invitrogen (Carlsbad, CA, USA). Mouse anti-NeuN antibody was obtained from Abcam (Cambridge, UK). Rabbit anti-glial fibrillary acidic protein (GFAP) antibody was purchased from Cell Signaling Technology (Danvers, MA, USA), and rabbit anti-IBL-1 antibody was purchased from Wako Chemicals (Osaka, Japan). Goat anti-Mouse IgG (H+L) Highly Cross-Adsorbed Secondary Antibody, Alexa Fluor 594, and Goat anti-Rabbit IgG (H+L) Highly Cross-Adsorbed Secondary Antibody, Alexa Fluor 488, were obtained from Thermo Fisher Scientific (Waltham, MA, USA). AffiniPure Goat Anti-Rabbit secondary antibody was purchased from Jackson ImmunoResearch (West Grove, PA, USA).

Model Preparation

To detect the roles of actin dynamics during the critical period of ocular dominance plasticity, we used the MD model. As the rats' eyes were not yet open at postnatal day (P)13, we performed lid suturing at this time point. The rats were anesthetized, and the MD model was generated by sewing the lid of the right eye of each rat with 6-0 silk. Eyelid closure was examined daily until complete healing had occurred. On P45, the V1 regions of the normal control and MD groups were evaluated by transmission electron microscopy (TEM) or synaptosome analysis. To detect changes in actin dynamics during visual cortical development, the visual cortex in another set of normal control rats was examined on P15, P30, and P45. To detect the effects of actin dynamics on the development of behavioral visual acuity, the inhibitor cytochalasin D was microinjected into the bilateral V1 from P33 to P45 once every 3 days for a total of five times. To test whether the visual acuity of the MD eye could be improved by the actin stabilizer jasplakinolide, after the right eyelids were subjected to MD on P13 jasplakinolide was administered into the V1 of the left hemisphere from P33 to P45 once every 3 days for a total of five times.

Tissue Preparation and TEM Data Analysis

Based on previous reports, we applied a three-step localization method to precisely locate the visual cortex.[5,6,18] The monocular area of the V1 (V1M) was recognized according to anatomical landmarks. A 3-mm-long V1M tissue block with a top of 1 mm^2 was dissected. Each long side of the tissue block contained cortical layers I to VI. After post-fixation, staining with osmium tetroxide, and dehydration, the tissue block was embedded. Sections (2-µm thick) were cut from one of the long sides of the embedded tissue block and stained with toluidine blue for histological localization. Histological staining of the semithin sections also showed all layers of the visual cortex. Serial 70-nm-thick ultrathin sections adjacent to the 2-µm histological sections were applied for ultrastructural localization. Visual fields for statistical analysis were chosen in the areas around pyramidal neurons in cortical layers IV and V (Supplementary Fig. S1).

Consecutive 70-nm-thick sections were cut and gathered on a single-slot grid for photography and analysis. Ten noncontiguous photographs were taken of sections from each animal at 10,000× magnification for quantification. Each photograph contained genuine neuropil regions of at least 250 μm^2. Synapses were defined, and statistical analyses were performed on synaptic density based on definitions from previous studies.[6,19,20] The method of N_A/d (where N_A is the number of synaptic profiles per unit area and d is the average cross-sectional length of synaptic junctions) is an assumption-based method for synaptic density statistics that can deduce three-dimensional synaptic density from the synapse number observed per unit area.[19–21] The average synaptic density from 10 visual fields derived from each V1M was considered the synaptic density of each animal. Normal mitochondria containing an outer membrane, inner membrane, and cristae were included in the statistical analysis. The average mitochondrial area percentage for all visual fields of each rat was defined as a percentage for each rat. Data analysis was performed with ImageJ software (National Institutes of Health, Bethesda, MD, USA). Each group contained at least three animals.

Synaptosome Preparation and Western Blot Analysis

Immediately after the rat brains had been removed at the designed time points, coronal brain sections were generated with the help of a matrix (RWD Life Science, Guangdong, China). Based on anatomic location,[22] V1 tissue blocks were obtained and frozen in liquid nitrogen. Before synaptosomal extraction, all tissues were kept at –80°C. Synaptosomal extraction and actin separation were performed as described in previous reports.[6,8,23] Briefly, synaptosomes, as an organelle, were isolated by sucrose differential centrifugation. The separation of synaptosomal polymerized filamentous actin (F-actin) and monomeric actin (G-actin) was based on the fact that the reactions of F-actin or G-actin to detergent at different strengths differ. G-actin is soluble in 1% Triton X-100, whereas F-actin is not; however, F-actin is soluble in 1% SDS. Therefore, synaptosomal F-actin and G-actin were separated by centrifugation. Each sample for

Investigative Ophthalmology & Visual Science

western blot analysis contained the V1s of seven rats without distinguishing between V1M and V1B. No fewer than three samples were analyzed for each group.

Electrophoresis on 10% sodium dodecyl sulfate–polyacrylamide gel electrophoresis (SDS-PAGE) gels was carried out for 45 minutes. Proteins were then transferred to a polyvinylidene fluoride membrane at 110 V at 4°C for 1.5 hours (Bio-Rad Laboratories, Hercules, CA, USA). The details of the western blot experiment were as follows: incubation with 5% nonfat milk for 1 hour, incubation with primary antibodies against actin (1:1000) or GAPDH (1:14,000) for over 16 hours at 4°C, and incubation with secondary antibodies (1:5000) for 1 hour at 25°C, after which primary and secondary antibodies were removed by washing three times in Tris-buffered saline with 0.1% Tween 20 detergent (TBST), and proteins were identified via an enhanced chemiluminescent system (MilliporeSigma, Burlington, MA, USA). The immunopositive bands were scanned and quantified using ImageJ software. The total actin immunoreactivity and F-actin/G-actin ratio on P15 were set at 1.0, and the levels at P30 and P45 were normalized to the relevant values at P15. To discover the effect of MD on actin dynamics, the level at P45 was set as 1.0, and values in the MD eye and MD fellow eye groups were normalized to the relevant values at P45. To discover the effects of cytochalasin D or jasplakinolide treatment on actin dynamics, the level in the vehicle group was set at 1.0, and the levels in the groups administered cytochalasin D or jasplakinolide were normalized to the relevant values in the vehicle group.

Surgical Procedures and Microinjection

SD rats (30 days old) were anesthetized, trained in a RWD 8001 stereotaxic apparatus (RWD Life Science), and surgically implanted with unilateral or bilateral guide cannulas to the visual cortex, depending on the behavioral procedure; coordinates relative to the bregma were anteroposterior (AP), –6.0 mm; lateral (L), ±3.0 mm; and ventral (V), –1.0 mm.[22] The first target microinjections were carried out after 3 days of recovery. One microliter of cytochalasin D (125 ng/µL) or jasplakinolide (20 ng/µL) was injected into the V1 with a microinfusion pump (KD Scientific, Holliston, MA, USA) at the designated times. The animals were fixed and subjected to microinjections under conscious conditions without anesthesia. Infusion was carried out at a rate of 1.0 µL/min.

Behavioral Visual Acuity Test

Behavioral visual acuity was assessed on P45 by applying the visual water maze task according to the protocol in a previous article.[24] A two-channel water maze containing two computer-controlled monitors at the end of each arm served as the basic setup. Grates with various spatial frequencies and a gray field were chosen as visual stimuli. The two stimuli randomly appeared on one of the two monitors. A transparent acrylic escape platform was immersed under the water below the monitor showing the grate. Rats were trained to associate swimming to the platform with escape from the water. The rats were trained to differentiate a vertical grate with a spatial frequency of 0.1 cycles per degree from the gray field and to correlate the transparent acrylic escape platform with the grate. The limits of the rats' recognition of gates with a higher spatial frequency were explored. Visual acuity was designated as the spatial frequency at which 70% of choices were correct.[24]

Immunofluorescence Histochemical Analysis

SD rats, 30-days old, were randomly divided into vehicle and cytochalasin D groups. The rats were fixed with a stereotactic apparatus after respiratory anesthesia (RWD Life Science). Based on the coordinates (AP, –6.0 mm; L, ±3.0 mm; and V, –1.0 mm), the catheter was transplanted into the V1. From P33 to P45, a WPI microinjection syringe pump (World Precision Instruments, Sarasota, FL, USA) was used to microinject cytochalasin D (125 ng/µL in normal saline and 1% DMSO) or vehicle (saline containing 1% DMSO). The dose at each side was 1 µg. The speed of administration was 300 nL/min. The drug was kept for 3 minutes after each administration. The frequency of administration was once every 3 days and was given a total of five times. Perfusion was performed 1 hour after the last administration. The anesthetized rats were perfused with 0.9% NaCl and then with 4% paraformaldehyde in 0.1-M PBS. The brain was stored in 4% paraformaldehyde for 6 to 8 hours at 4°C, then transferred to 30% sucrose with 0.1-M PBS and stored at 4°C for 5 to 7 days. Based on anatomic location, the position of the visual cortex in the coronal plane of the brain was determined, and 40-µm-thick slices were cut using a freezing sliding microtome (Leica, Wetzlar, Germany); one coronal slice was collected every 240 µM. There were no fewer than eight slices in each set of slices of visual cortex. A similar set of brain slices was taken for immunofluorescence analysis in the vehicle or cytochalasin D groups.

After three times of washing with TBS, the brain slices were incubated in the block solution, which contained 10% goat serum and 0.3% Triton X-100 at room temperature for 2 hours. Next, the slices were incubated with rabbit anti-GFAP antibody (1:200) or mouse anti-NeuN antibody (1:1000) at 4°C for 24 hours or with rabbit anti-IBL-1 antibody (1:100) at 4°C for 48 hours. Then, after washing three times in TBS, the sections for GFAP and Ionic calcium Binding Adaptor molecule-1 (IBA-1) immunohistochemistry detection were incubated with Alexa Fluor 488-conjugated Goat anti-Rabbit Secondary Antibody (1:100) at room temperature for 3 hours. The sections for NeuN detection were incubated with Alexa Fluor 594-conjugated Goat anti-Mouse Secondary Antibody (1:500) at room temperature for 2 hours. The slices were washed three times with TBS and attached to the glass slides. Then, the anti-fluorescence quenching agent was added to the slide, and the cover glass was covered. According to the cortical anatomic location, V1M and V1B of both sides were analyzed via fluorescence microscope (Olympus, Tokyo, Japan). The visual field was selected in the middle of each V1M or V1B region and photographed under a fluorescence microscope. Each side (left or right) of the brain region (V1M/V1B) in a rat was taken as one sample. No fewer than eight photographs within each sample and no fewer than 32 photographs of each animal were taken. The percentage of the antibody positive-expression regions of each photograph was calculated using the Nikon NIS-Elements AR image analysis software. The average of all of the photographs in each side of the brain area of each animal was the value of this sample. SPSS Statistics 17.0 (IBM, Armonk, NY, USA) was used to analyze the data FOR THE two groups of animals. Representative photos were also taken under the confocal laser scanning microscope (Carl

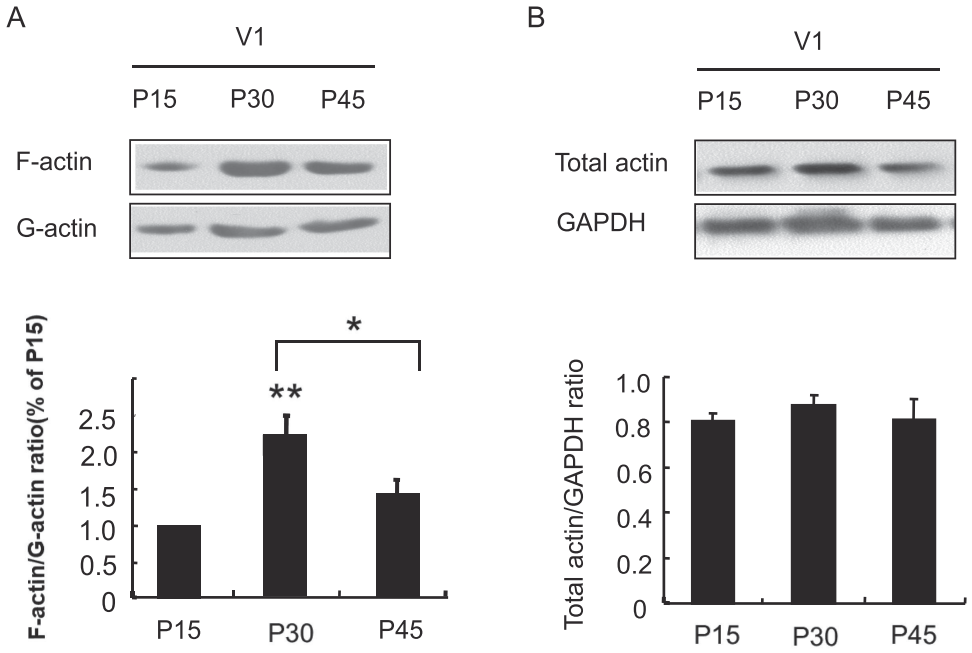

Figure 1. Alterations in synaptosomal actin dynamics during visual cortical development. (**A**) The levels of synaptosomal F-actin/G-actin in the V1 during visual development (on P15, P30, and P45) determined by immunoblotting. (**B**) Effect of development on total synaptosomal actin expression. Statistical values are shown as the mean ± SEM. At least three samples from each group were assessed. Each sample consisted of the visual cortices of seven rats ($^{**}P < 0.01$ vs. P15 group; $^{*}P < 0.05$ vs. P30 group).

Zeiss, Jena, Germany) in Experimental Center of Shandong University of Traditional Chinese Medicine.

Statistical Analyses

Statistical analyses of the data were carried out via SPSS Statistics 17.0. Statistical significance was evaluated by *t*-test or one-way analysis of variance. All parameters are described as the mean ± SEM. Differences for which $P < 0.05$ were considered statistically significant.

Results

Alterations in Actin Dynamics, Synaptic Density, and Mitochondrial Area During Visual Cortical Development

A previous electron microscopic study demonstrated that synaptic densities within the visual cortices of rats increased dramatically over the first 4 postnatal weeks and remained stable until P90.[10] Similarly, it was also reported that the total concentration of F-actin in the visual cortex peaks at approximately P30.[11] Nonetheless, few experimental studies have simultaneously explored these two indices.

Actin, the primary element of synaptic filaments in the spine head, and actin dynamics play essential roles in synaptic plasticity.[2–8] Whether actin dynamics regulate synapse formation during visual cortical development is still not well known. We first quantitatively investigated changes in the equilibrium between synaptosomal polymerized F-actin and monomeric G-actin in the V1 (both the V1M and V1B). Figure 1A demonstrates that the normalized F-actin/G-actin ratio in the V1 reached its highest value at P30. Interestingly, after reaching an inflection point at P30, this ratio was significantly decreased on P45, $F_{(2, 6)} = 7.550$, $P < 0.05$ (post hoc analysis, P30 vs. P15, $P < 0.01$; P45 vs. P30, $P < 0.05$). To exclude the possibility that these alterations were derived from changes in actin expression, total actin expression was also investigated. The levels of total actin did not change significantly during visual development, indicating that the balance between F-actin and G-actin, but not actin protein expression, changed during postnatal visual development (Fig. 1B).

In rodents, the V1M receives visual messages from the contralateral eye and responds to stimulation of the peripheral visual field, whereas the binocular response area (V1B) receives visual input from both eyes and responds to stimulation of the central area of the visual field.[25,26] We analyzed the density of synapses in the V1M on P15, P30, and P45, which showed an increased synaptic density on P30 and P45 compared with P15. However, the synaptic density between P30 and P45 remained stable, $F_{(2, 8)} = 22.366$, $P < 0.01$ (post hoc analysis, P30 vs. P15, $P < 0.01$; P45 vs. P15, $P < 0.01$) (Fig. 2). The synaptic density within the V1B (cortical layers IV–V) between P30 and P45 also illustrated no significant difference.[18]

In addition to its role as an essential building block for synapse formation, actin is also located at the spine neck, where it promotes efficient synaptic transmission via regulation of the speed with which neurotransmitter receptors relay messages to the postsynaptic membrane.[27–29] The degree of actin dynamics also reflects the functions of neurotransmitters and proteins at synapses. Mitochondria are closely related to synaptic function, and, to some extent, their content can reflect the plasticity of synapses. The area of normal mitochondria under TEM can also be used as an index of mitochondrial function under physiological or pathological conditions.[30–35] To clarify alterations

Investigative Ophthalmology & Visual Science

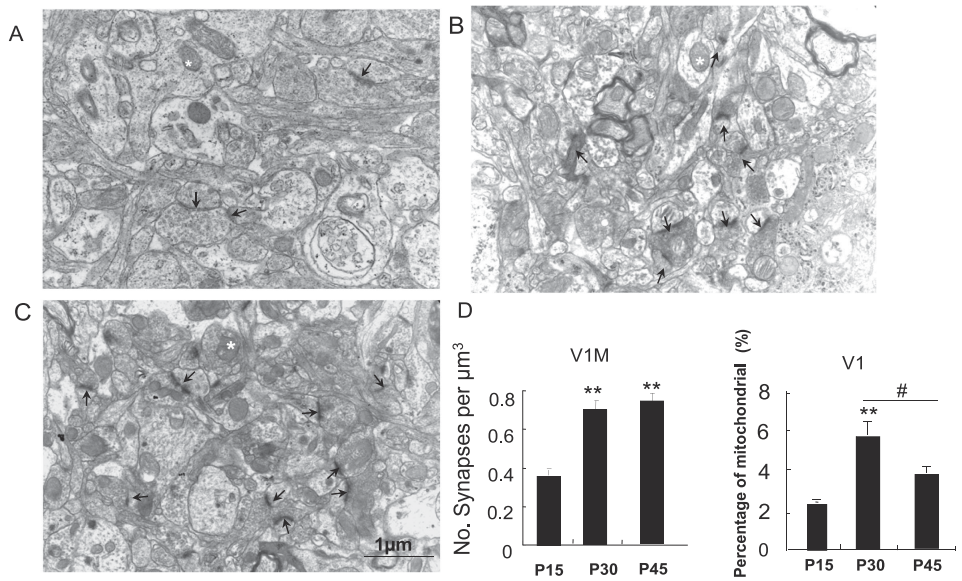

Figure 2. Alterations in synaptic density and mitochondrial area in the V1M during visual cortical development are shown. (**A–C**) TEM images demonstrating synapses and mitochondria in layers IV and V of the V1M on P15, P30, and P45. *Black arrows* indicate synapses, and a *white asterisk* in each photograph indicates a mitochondrion. (**D**) Statistical analysis of synaptic density and mitochondrial area. Statistical values are shown as the mean ± SEM; $n = 3$ to 7 for each group ($^{**}P < 0.01$ vs. P15 group).

in actin dynamics and synaptic density from P30 to P45, we analyzed changes in the mitochondrial area during visual development. Interestingly, the mitochondrial area also increased and showed an inflection point at approximately P30, $F_{(2, 6)} = 18.810$, $P < 0.01$ (post hoc analysis, P30 vs. P15, $P < 0.01$; P45 vs. P15, $P < 0.05$; P45 vs. P30, $P < 0.05$) (Fig. 2), which was consistent with the pattern of changes in actin dynamics. The above results demonstrated that synaptosomal actin dynamics may be related to synaptic structure and function within the visual cortex.

Actin Dynamics Are Essential for the Development of Behavioral Visual Acuity

The above experiments demonstrated that actin dynamics, synaptic density, and mitochondrial area in the V1 increased during a critical period; however, the question of whether actin dynamics regulate structural and functional synaptic plasticity during visual development still required further investigation, as well as determining whether actin dynamics are essential to the degree of visual acuity. To answer these questions, cytochalasin D was injected into the V1 from P33 to P45. Cytochalasin D functions by binding the polymerizing end of F-actin and decreasing the polymerization and depolymerization rates.[30] Cytochalasin D was administered by microinjection once every 3 days for a total of five times. At this dose, the drug did not disrupt or break down the existing circuits, including dendrites and axons.[5–7,31] After the administration of cytochalasin D five times, the rats' visual acuity was quantitatively assessed in the visual water maze. The behavioral visual acuity experiments were designed based on a previous report.[24] As demonstrated in Figure 3, analysis of the behavioral visual acuity data by *t*-test revealed a significant reduction in visual acuity in the cytochalasin D–treated group compared with the vehicle control group, $t_{(8)} = 4.785$, $P < 0.05$. This result suggests that actin dynamics correlate with changes in visual acuity during the period of development of binocularity. To investigate whether actin dynamics regulate structural and functional synaptic plasticity during visual development, the visual cortices of vehicle-treated and cytochalasin D–treated animals were collected for western blot analysis. As demonstrated in Figure 4A, cytochalasin D injection significantly reduced the synaptosomal F-actin/G-actin ratio within the visual cortex, $t_{(4)} = 10.594$, $P < 0.01$; however, the total actin levels showed no significant difference. Furthermore, the V1M regions of the vehicle- and cytochalasin D–injected animals were collected for TEM analysis, which revealed a significant reduction in synaptic density and mitochondrial area within the V1M of the cytochalasin D–injected rats: synaptic density, $t_{(6)} = 3.555$, $P < 0.05$; mitochondrial area, $t_{(4)} = 3.5$, $P < 0.05$ (Fig. 4B). To make it clear whether the treatment with cytochalasin D could degrade visual acuity, synaptic density, and mitochondrial area through some cytotoxic/inflammatory mechanisms, cytochalasin D or vehicle was microinjected into the V1 of the different sets of rats from P30 to P45. At P45, the brains were dissected for immunofluorescence histochemical analysis of the NeuN-positive neurons, GFAP-positive astrocytes, and IBA-positive microglia. It showed that there were no significant differences between the vehicle and cytochalasin D groups in the area percentage of the NeuN-, GFAP-, and IBA-positive cells, whether in the V1M or V1B: neurons in the V1M, $t_{(5)} = 0.787$, $P > 0.05$; astrocytes in the V1M, $t_{(5)} = -0.742$, $P > 0.05$; microglia in the V1M, $t_{(5)} = -2.132$, $P > 0.05$; neurons in the V1B, $t_{(5)} = -1.923$, $P > 0.05$; astrocytes in the V1B, $t_{(5)} = 0.078$, $P > 0.05$; microglia in the V1B, $t_{(5)} = -1.332$, $P > 0.05$ (Fig. 5). The results indicated that microinjection of cytochalasin D (125 ng/μL, 1 μL) could not induce cytotoxicity or inflammation within the primary visual cortex. All of the above results indicated that actin dynamics correlated with synaptic changes in V1, and elimination of these actin changes plays a role in the development of visual acuity during this critical time period.

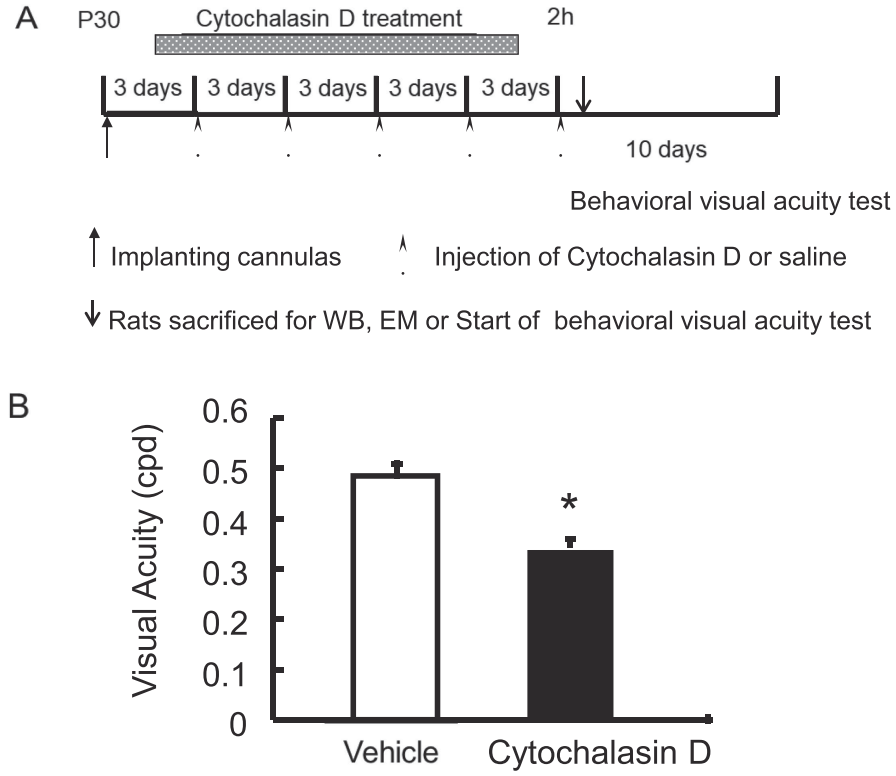

Figure 3. Actin dynamics are necessary for the development of behavioral visual acuity during visual development. (**A**) Schematic of the experimental design. (**B**) Microinjection of cytochalasin D (125 ng per visual cortex) into the binocular visual cortex on P30 to P45 prevented the development of behavioral visual acuity. Statistical values are shown as the mean ± SEM; $n = 3$ to 5 for each group ($^{*}P < 0.05$ vs. vehicle-treated group).

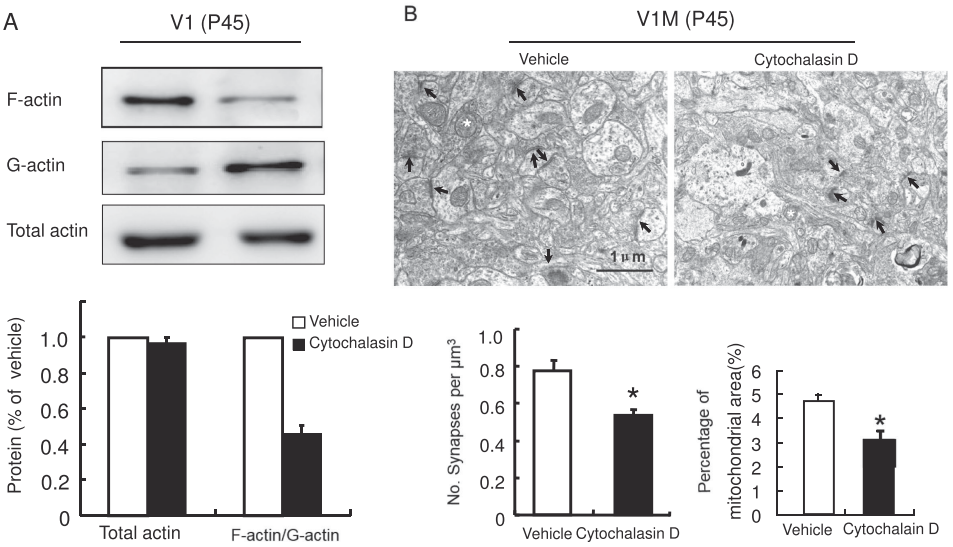

Figure 4. Actin dynamics regulate structural and functional synaptic plasticity in the visual cortex. (**A**) Western blot analysis of synaptosomal total actin and F-actin/G-actin in the V1 of vehicle-treated or cytochalasin D–treated animals. Statistical values are shown as the mean ± SEM. At least three samples from each group were assessed. Each sample consisted of the visual cortices of seven rats. (**B**) Representative visual fields illustrate synaptic density and mitochondrial area in the V1M of the vehicle-treated and cytochalasin D–treated groups. *Black arrows* indicate synapses, and a *white asterisk* in each photograph indicates a mitochondrion. Statistical values are shown as the mean ± SEM. Each group consisted of three to four rats ($^{*}P < 0.05$, $^{**}P < 0.01$ vs. vehicle group).

Investigative Ophthalmology & Visual Science

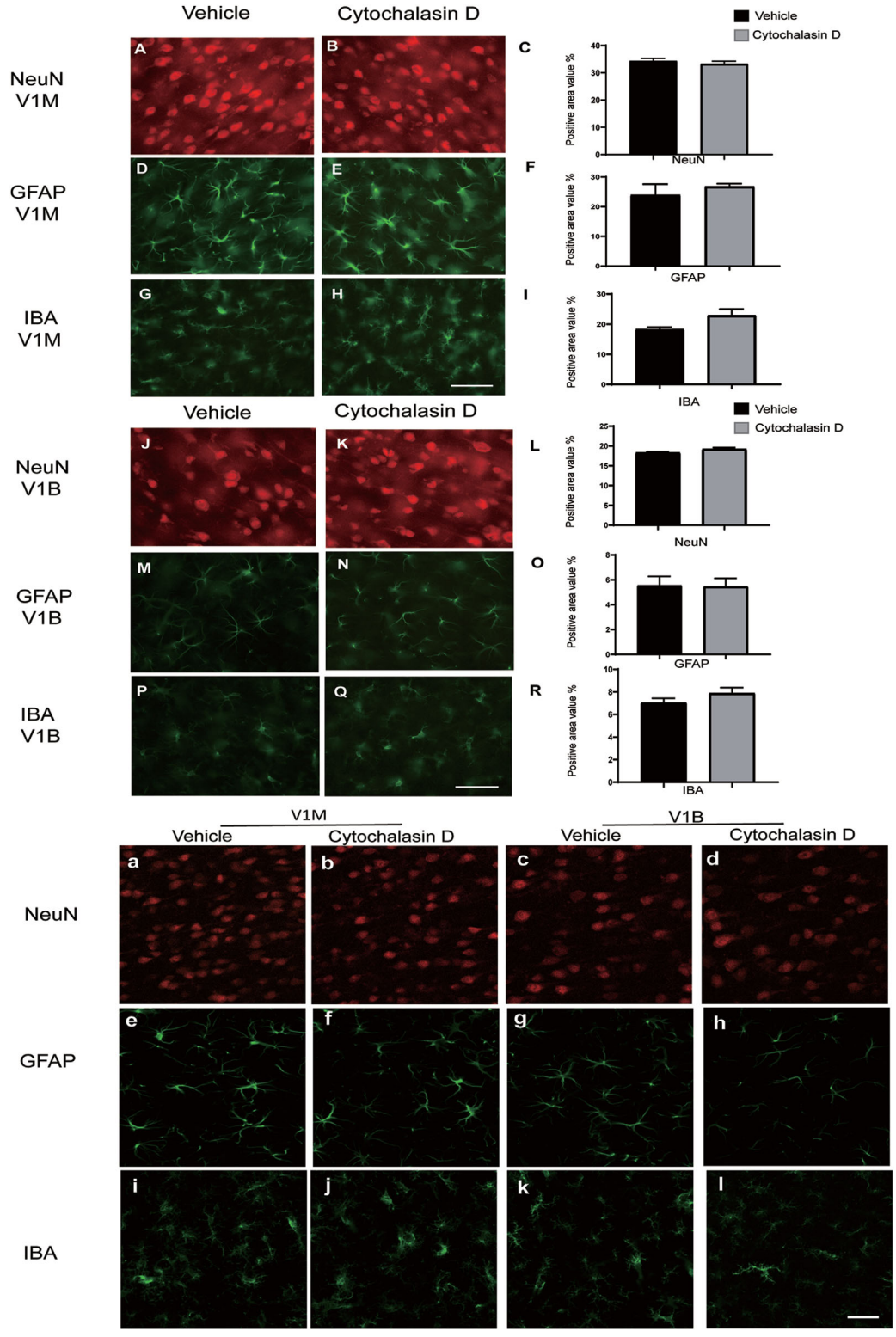

Figure 5. Alterations in the quantity of neurons, astrocytes, and microglia in the V1 of rats after vehicle or cytochalasin D microinjection from P30 to P45. (**A–R**) Fluorescence microscopy showed changes in the number of neurons, astrocytes, and microglia in the V1 of two groups of rats. Shown are NeuN-positive neurons (**A–C**), GFAP-positive astrocytes (**D–F**), and IBA-positive microglia (**G–I**) in the V1M of rats after being microinjected with vehicle or cytochalasin D. Alterations in the neurons (**J–L**), astrocytes (**M–O**), and microglia (**P–R**) are shown in the V1B of rats after being injected with vehicle or cytochalasin D. Statistical values are shown as the mean ± SEM; $n = 6$ for each group. (**a–d**) Representative confocal laser scanning microscope images of neurons in the V1M and V1B in the vehicle- or cytochalasin D–microinjected group. (**e–h**) Representative confocal laser scanning microscope images of astrocytes in the V1M and V1B in the vehicle control and cytochalasin D groups. (**i–l**) Representative visual fields of microglia in the V1M and V1B observed under confocal laser scanning microscope. *Scale bars*: 50 µm.

Investigative Ophthalmology & Visual Science

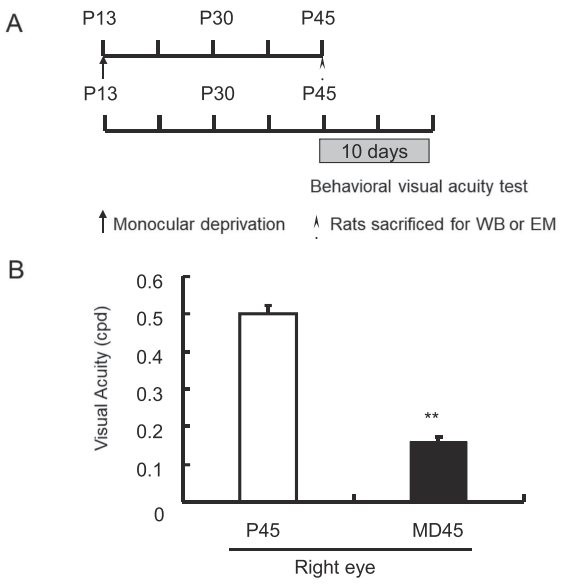

Figure 6. Effect of MD on behavioral visual acuity. (**A**) Schematic of the experimental design. (**B**) MD from P13 to P45 reduced the visual acuity of the deprived eye compared with the control eye in the P45 control group. Statistical values are shown as the mean ± SEM. Each group consisted of seven to eight rats ($^{**}P < 0.01$ vs. P45 group).

MD Altered Actin Dynamics-Related Changes in Synaptic Structure and Function in the Bilateral Visual Cortex

Amblyopia is a disease closely related to visual development. Because the above experiment showed that synaptosomal actin dynamics play a role in the development of visual acuity, whether actin dynamics-related structural and functional plasticity is involved in the development of amblyopia remained unknown. Next, we explored this possibility using a long-term MD model.[32,36–40] The right eyelids of the rats were sutured shut on P13 and reopened on P45, and behavioral visual acuity of the right eye was tested. As shown in Figure 6, analysis of the behavioral visual acuity data by *t*-test revealed a significant reduction in visual acuity in the right eye at P45 in the monocular deprivation group compared with the control group, $t_{(13)} = 13.471$, $P < 0.01$. As MD caused a decrease in visual acuity, we wondered whether it affected actin dynamics, the mitochondrial area, or synaptic density in the visual cortex. Different groups of rats were chosen and used to analyze actin dynamics and ultrastructural changes. Interestingly, as illustrated in Figure 7A, the synaptosomal F-actin/G-actin ratio in the V1 contralateral to the deprived eye at P45 was not significantly different from that in the control group. However, MD significantly decreased actin dynamics in the visual cortex contralateral to the deprived eye compared with those in the nondeprived eye in the same animal. In addition, the F-actin/G-actin ratio in the visual cortex contralateral to the nondeprived eye at P45 was significantly higher than that in the control group, $F_{(2, 6)} = 8.788$, $P < 0.05$ (post hoc analysis, MD eye vs. MD fellow eye group, $P < 0.01$; MD fellow eye vs. control group at P45, $P < 0.05$). The V1M regions contralateral or ipsilateral to the deprived eye were also collected for TEM analysis, which revealed a significant decrease in the synaptic density and mitochondrial area in the V1M contralateral to the deprived eye compared with that contralateral to the fellow eye: synaptic density of nondeprived eye, $t_{(4)} = 3.808$, $P < 0.05$; mitochondrial area, $t_{(4)} = -4.426$, $P < 0.05$ (Fig. 7B).

Stabilization of Actin Polymerization Promoted the Recovery of Visual Acuity in Amblyopic Rats and Increased Actin Dynamics, Mitochondrial Area, and Synaptic Density in the V1 Driven by the Deprived Eye

Because long-term MD decreased actin dynamics and synaptic plasticity in the visual cortex contralateral to the deprived eye compared with that contralateral to the nondeprived eye (ipsilateral to the deprived eye), conversely, could a pharmacological-induced increase in actin polymerization reverse these synaptic alterations? Moreover, because an actin polymerization inhibitor reduced visual acuity, could jasplakinolide, an agent that stabilizes actin polymerization, improve visual acuity in the deprived eye?[41,42] To address these questions, the right eyelids of the rats were sutured shut on P13, and on P30 jasplakinolide or vehicle was microinjected into the V1 of the left hemisphere of rats in the two groups. Microinjection was conducted once every 3 days for a total of five times. Jasplakinolide prevents filament depolymerization and shifts the equilibrium from monomer toward filaments.[43–45] The dose of jasplakinolide mentioned in this manuscript has been proven to improve learning and memory abilities of rats and mice via stabilization of actin filaments.[6,42] On P45, the eyelids were reopened, and behavioral visual acuity in each eye was tested. As shown in Figure 8, data from the MD + vehicle group and MD + jasplakinolide group illustrated that visual acuity of the MD eye was significantly decreased compared with that of the fellow eyes. However, jasplakinolide microinjection significantly improved visual acuity in amblyopic eyes compared with vehicle-treated MD control eyes, $F_{(3, 16)} = 105.635$, $P < 0.01$ (post hoc analysis, MD eye vs. fellow eye in the MD + vehicle group, $P < 0.01$; MD eye vs. fellow eye in the MD + jasplakinolide group, $P < 0.01$; MD eye in the MD + vehicle group vs. MD eye in the MD + jasplakinolide group, $P < 0.01$). To determine whether jasplakinolide could rescue the decreases in actin filament polymerization, the mitochondrial area, and synaptic density within the V1 during long-term MD, the V1 tissue of vehicle- and jasplakinolide-treated amblyopic animals was taken 2 hours after the last microinjection for analysis of synaptosomal actin dynamics through western blot assay. As shown in Figure 9A, jasplakinolide injection induced a significant increase in the synaptosomal F-actin/G-actin ratio, $t_{(4)} = 15.790$, $P < 0.01$. The V1M areas of rats in the MD + vehicle and MD + jasplakinolide groups were also taken for TEM analysis, which showed that the synaptic density and mitochondrial area in the V1M of the jasplakinolide-treated group were significantly increased: synaptic density, $t_{(6)} = 4.005$, $P < 0.01$; mitochondrial area, $t_{(8)} = -4.651$, $P < 0.01$ (Fig. 9B). These results showed that the injection of an actin polymerization stabilizer partly improved visual acuity in the amblyopic eye and increased synaptic density and mitochondrial area in the V1 driven by the deprived eye, suggesting that actin dynamics regulate structural and functional synaptic plasticity and contribute to the formation of amblyopia.

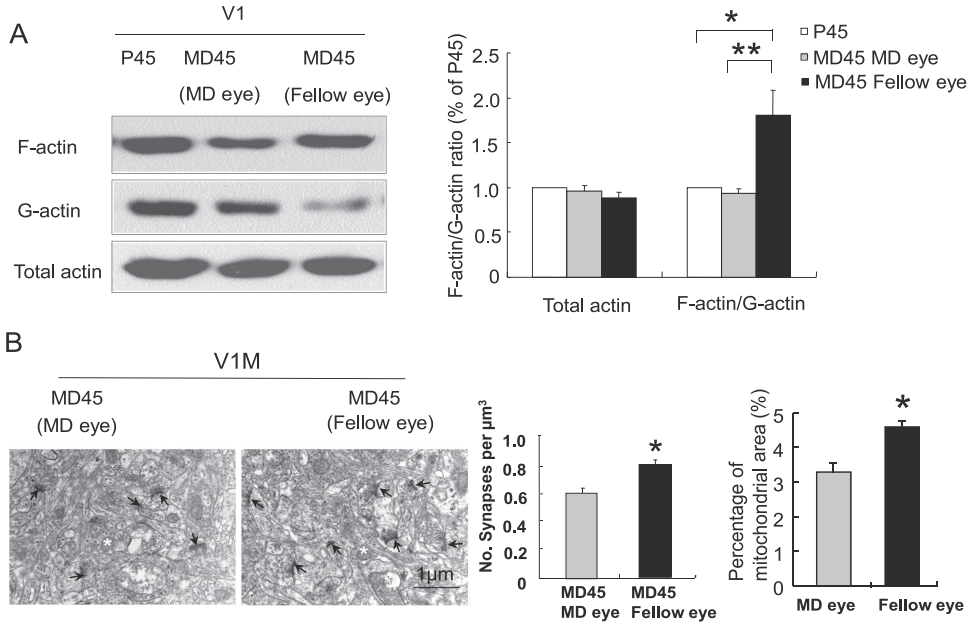

Figure 7. Effects of MD on actin dynamics, synaptic density, and mitochondrial area in the V1. (**A**) Total synaptosomal actin and the F-actin/G-actin ratio in the V1 at P45 in the control group, cortex contralateral to the amblyopic eye (MD eye), and cortex contralateral to the fellow (nonamblyopic) eye (fellow eye) were determined by immunoblotting. Statistical values are shown as the mean ± SEM; $n = 3$ for each group. Each sample contained V1 tissue from seven rats ($^{**}P < 0.01$ vs. MD eye group). (**B**) Representative TEM image demonstrating synapses and mitochondria in cortical layers IV and V of the V1M driven by the MD eye and fellow eye. Synapses are indicated by *arrows*. In each photograph, a representative mitochondrion is indicated by a *white asterisk*. *Scale bar*: 1 μm. The synaptic densities in the V1M driven by the MD eye and the fellow eye were estimated. Statistical values are shown as the mean ± SEM. At least three samples from each group were assessed ($^{*}P < 0.05$ vs. MD eye group).

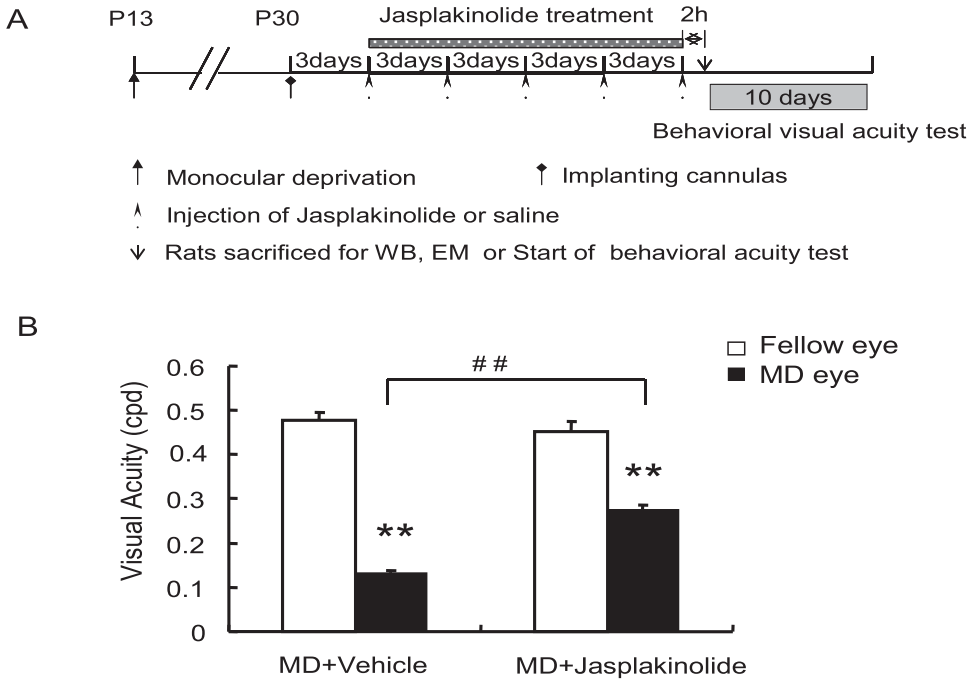

Figure 8. Stabilization of actin polymerization partly improved visual acuity in the amblyopic eye. (**A**) Schematic of the experimental design. (**B**) Behavioral visual acuity was detected after microinjection of jasplakinolide or vehicle into the V1 driven by the deprived eye. Statistical values are shown as the mean ± SEM; $n = 5$ for each group ($^{\#\#}P < 0.05$ vs. MD + vehicle group; $^{**}P < 0.05$ vs. fellow eye group).

Investigative Ophthalmology & Visual Science

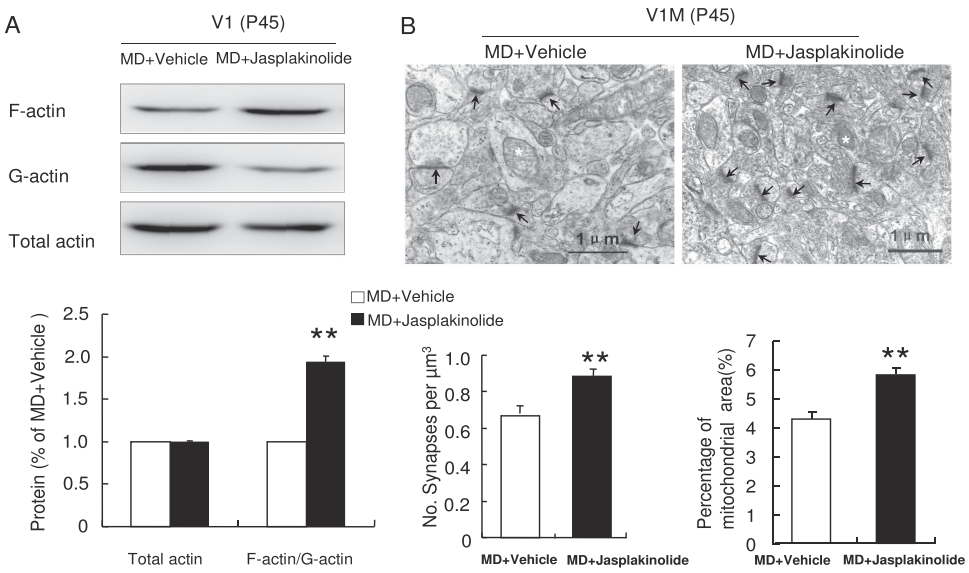

Figure 9. Stabilization of actin polymerization partly increased the synaptic density and mitochondrial area in the V1M contralateral to the deprived eye. (**A**) Western blot analysis showing the normalized levels of synaptosomal total and F-actin/G-actin ratios in the V1 of the MD + vehicle and MD + jasplakinolide groups. Statistical values are shown as the mean ± SEM. At least three samples from each group were assessed. Each sample consisted of the visual cortices of seven rats. (**B**) Representative visual fields illustrate synapses and mitochondria in the V1M of cortical layers IV and V of the MD + vehicle and MD + jasplakinolide groups. *Black arrows* indicate synapses, and a *white asterisk* in each photograph indicates a mitochondrion. Statistical values are shown as the mean ± SEM; $n = 3$ to 5 for each group ($^{**}P <$ 0.01 vs. MD + vehicle group).

Discussion

The present study provides a new perspective on the roles of actin dynamics in development of the visual cortex and the pathogenesis of amblyopia.

First, we found that actin dynamics regulate synapse formation, reflect functional synaptic plasticity in the visual cortex, and are required for the development of visual acuity. Actin dynamics are essential for synaptic function and play important roles in the stages of learning and memory.[5–9] Previous reports have demonstrated actin dynamics and synaptic alterations in the visual cortex.[10,11] However, whether synaptosomal actin dynamics regulate synaptic plasticity or play a role in visual function has not been thoroughly investigated. In the present study, injection of an actin polymerization inhibitor into the V1 significantly decreased synaptic density, demonstrating that actin dynamics are an upstream regulator of synaptic density during visual development. Moreover, cytochalasin D microinjection into the V1 significantly impaired behavioral visual acuity. Interestingly, during the specific period from postnatal day 30 to 45, synaptosomal actin dynamics and synaptic density were differentially altered, indicating that alterations in synaptic density and actin dynamics do not follow the same trend.[18] Here, we further found that actin dynamics and mitochondrial area within the axon and dendrite terminals of neurons are related. Mitochondria are energy factories that provide adenosine triphosphate for cellular activities. Actin polymerization and depolymerization themselves require energy. In addition, the dynamics of actin in the spine neck can promote the movement of functional proteins to the synaptic membrane, which also requires energy provided by mitochondria. Actin dynamics and mitochondrial area may occur simultaneously but not show a causal relationship. However, cytochalasin D microinjection into the V1 significantly decreased the mitochondrial area, indicating that, to some extent, a change in the mitochondrial content in nerve endings can reflect actin dynamics-related functional synaptic plasticity. The time at which actin dynamics peak, P30, may represent the peak of functional synaptic plasticity during the critical period of visual development in rats.

Second, we demonstrated that actin dynamics-related synaptic plasticity contributes to amblyopia formation. The monocular deprivation model is not only the gold standard for modeling amblyopia but also a classical model for the study of ocular dominance plasticity. Although ocular dominance plasticity has been widely studied, and some molecules and molecular mechanisms, including NMDA receptors, GABA, neurotrophic factors, intracellular signaling pathways, extracellular matrix, and gene regulation,[12–16,46–51] have been demonstrated to participate in this type of plasticity, synaptic plasticity of the visual cortex at the ultrastructural level and its related molecular mechanisms have not been thoroughly investigated. In the present study, we found that MD induced significant decreases in synaptosomal actin dynamics, the mitochondrial area, and synaptic density in the visual cortex contralateral to the amblyopic eye compared with that contralateral to the nonamblyopic eye and impaired behavioral visual acuity. The actin polymerization stabilizer jasplakinolide partly increased actin dynamics, the mitochondrial area, and synaptic density, as well as visual acuity. These results suggest that during the development of amblyopia, actin dynamics-related structural synaptic density decreases, resulting in a deficit in visual acuity. The actin dynamics-related parameters of MD further provided evidence that actin dynamics are involved in visual cortical development, which is also activity dependent. A similar decrease in synaptic density during monocular deprivation has been reported.[52,53] MD was reported to decrease

the expression of cardiac troponin C, an upstream regulator of actin dynamics, in the mouse visual cortex driven by the deprived eye compared with the nondeprived eye, which is also consistent with our actin dynamics results.[53] Notably, no difference in actin dynamics at P45 between the visual cortex contralateral to the amblyopic eye and the normal eye was shown. This may have been because of compensation from the nonamblyopic eye in the V1B, during which responses from the closed eye are reduced, whereas responses from the open eye are enhanced.[54,55] Espinosa and Stryker speculated that 4 weeks of MD decreased responses from the deprived eye to the visual cortex but increased responses from the fellow eye. In addition, the connections in all cortical layers were increased.[56] Our present experimental results further indicated enhanced actin dynamics in cells responding to the nondeprived eye and binocular projections to the V1B from the nondeprived eye may have contributed to this absence of a difference between the visual cortex contralateral to the deprived eye and the normal control at P45.

Overall, we found that synaptosomal actin dynamics regulate structural and functional synaptic plasticity and play essential roles in the development of visual acuity. Notably, microinjection of the actin polymerization stabilizer jasplakinolide partly improved the changes in synaptic density and visual acuity in MD rats. In the future, the molecules that directly regulate actin dynamics in the visual cortex will be explored, and interventions at these novel targets may be useful as effective amblyopia treatments.

Acknowledgments

Supported by grants from the National Key Research and Development Project (2019YFC1710204), National Natural Science Foundation of China (31300907), Natural Science Foundation of Shandong Province (ZR2013HQ028), Key Development & Research Program of Shandong Province (2017CXGC1211, 2018JHZ005, and 2019GSF108252), and First-Class Disciplines of Shandong University of Traditional Chinese Medicine (220307), as well as funding from Shandong Provincial Key Laboratory of Integrated Traditional Chinese and Western Medicine for Prevention and Therapy of Ocular Diseases. We appreciated the help of the Ultrastructural Laboratory of the Shandong WEI-YA Biotech Company, and Experimental Center of Shandong University of Traditional Chinese Medicine.

Disclosure: **A.-L. Bi,** None; **Y.-Y. Zhang,** None; **Z.-Y. Lu,** None; **H.-Y. Tang,** None; **X.-Y. Zhang,** None; **Z.-H. Zhang,** None; **B.-Q. Li,** None; **D.-D. Guo,** None; **S. Gong,** None; **Q. Li,** None; **X.-R. Wang,** None; **X.-Z. Lu,** None; **H.-S. Bi,** None

References

1. Fukazawa Y, Saitoh Y, Ozawa F, Ohta Y, Mizuno K, Inokuchi K. Hippocampal LTP is accompanied by enhanced F-actin content within the dendritic spine that is essential for late LTP maintenance in vivo. *Neuron*. 2003;38:447–460.
2. Lin B, Kramar EA, Bi X, Brucher FA, Gall CM, Lynch G. Theta stimulation polymerizes actin in dendritic spines of hippocampus. *J Neurosci*. 2005;25:2062–2069.
3. Zhou Q, Homma KJ, Poo MM. Shrinkage of dendritic spines associated with long-term depression of hippocampal synapses. *Neuron*. 2004;44:749–757.
4. Zito K, Knott G, Shepherd GM, Shenolikar S, Svoboda K. Induction of spine growth and synapse formation by regulation of the spine actin cytoskeleton. *Neuron*. 2004;44:321–334.
5. Bi AL, Wang Y, Li BQ, et al. Region-specific involvement of actin rearrangement-related synaptic structure alterations in conditioned taste aversion memory. *Learn Mem*. 2010;17:420–427.
6. Bi AL, Wang Y, Zhang S, et al. Myosin II regulates actin rearrangement-related structural synaptic plasticity during conditioned taste aversion memory extinction. *Brain Struct Funct*. 2015;220:813–825.
7. Fischer A, Sananbenesi F, Schrick C, Spiess J, Radulovic J. Distinct roles of hippocampal de novo protein synthesis and actin rearrangement in extinction of contextual fear. *J Neurosci*. 2004;24:1962–1966.
8. Hou YY, Lu B, Li M, et al. Involvement of actin rearrangements within the amygdala and the dorsal hippocampus in aversive memories of drug withdrawal in acute morphine-dependent rats. *J Neurosci*. 2009;29:12244–12254.
9. Mantzur L, Joels G, Lamprecht R. Actin polymerization in lateral amygdala is essential for fear memory formation. *Neurobiol Learn Mem*. 2009;91:85–88.
10. Blue ME, Parnavelas JG. The formation and maturation of synapses in the visual cortex of the rat. I. Qualitative analysis. *J Neurocytol*. 1983;12:599–616.
11. Nona SN, Trowell SC, Cronly-Dillon JR. Postnatal developmental profiles of filamentous actin and of 200 kDa neurofilament polypeptide in the visual cortex of light- and dark-reared rats and their relationship to critical period plasticity. *FEBS Lett*. 1985;186:111–115.
12. Berardi N, Pizzorusso T, Ratto GM, Maffei L. Molecular basis of plasticity in the visual cortex. *Trends Neurosci*. 2003;26:369–378.
13. McAllister AK, Katz LC, Lo DC. Neurotrophins and synaptic plasticity. *Annu Rev Neurosci*. 1999;22:295–318.
14. Sur M, Nagakura I, Chen N, Sugihara H. Mechanisms of plasticity in the developing and adult visual cortex. *Prog Brain Res*. 2013;207:243–254.
15. Bear MF, Kleinschmidt A, Gu QA, Singer W. Disruption of experience-dependent synaptic modifications in striate cortex by infusion of an NMDA receptor antagonist. *J Neurosci*. 1990;10:909–925.
16. Hensch TK, Fagiolini M, Mataga N, Stryker MP, Baekkeskov S, Kash SF. Local GABA circuit control of experience-dependent plasticity in developing visual cortex. *Science*. 1998;282:1504–1508.
17. Shepherd JD, Bear MF. New views of Arc, a master regulator of synaptic plasticity. *Nat Neurosci*. 2011;14:279–284.
18. Chen MQ, Bi AL, Zhang YY, et al. Different patterns of changes between actin dynamics and synaptic density in the rat's primary visual cortex during a special period of visual development. *Brain Res Bull*. 2017;132:199–203.
19. Alonso-Nanclares L, Gonzalez-Soriano J, Rodriguez JR, DeFelipe J. Gender differences in human cortical synaptic density. *Proc Natl Acad Sci USA*. 2008;105:14615–14619.
20. Beaulieu C, Colonnier M. A laminar analysis of the number of round-asymmetrical and flat-symmetrical synapses on spines, dendritic trunks, and cell bodies in area 17 of the cat. *J Comp Neurol*. 1985;231:180–189.
21. Palomero-Gallagher N, Zilles K. Cortical layers: cyto-, myelo-, receptor- and synaptic architecture in human cortical areas. *NeuroImage*. 2019;197:716–741.
22. Paxinos G, Watson C. *The Rat Brain in Stereotaxic Coordinates*. 6th ed. Amsterdam: Elsevier Science; 2007.
23. Toda S, Alguacil LF, Kalivas PW. Repeated cocaine administration changes the function and subcellular distribution of adenosine A1 receptor in the rat nucleus accumbens. *J Neurochem*. 2003;87:1478–1484.
24. Prusky GT, West PW, Douglas RM. Behavioral assessment of visual acuity in mice and rats. *Vision Res*. 2000;40:2201–2209.

25. Adams AD, Forrester JM. The projection of the rat's visual field on the cerebral cortex. *Q J Exp Physiol Cogn Med Sci*. 1968;53:327–336.
26. Montero VM. Evoked responses in the rat's visual cortex to contralateral, ipsilateral and restricted photic stimulation. *Brain Res*. 1973;53:192–196.
27. Chiu SL, Cline HT. Insulin receptor signaling in the development of neuronal structure and function. *Neural Dev*. 2010;5:7.
28. Gu J, Lee CW, Fan Y, et al. ADF/cofilin-mediated actin dynamics regulate AMPA receptor trafficking during synaptic plasticity. *Nat Neurosci*. 2010;13:1208–1215.
29. Lei W, Omotade OF, Myers KR, Zheng JQ. Actin cytoskeleton in dendritic spine development and plasticity. *Curr Opin Neurobiol*. 2016;39:86–92.
30. Chodniewicz D, Alteraifi AM, Zhelev DV. Experimental evidence for the limiting role of enzymatic reactions in chemoattractant-induced pseudopod extension in human neutrophils. *J Biol Chem*. 2004;279:24460–24466.
31. Huang FY, Li YN, Mei WL, Dai HF, Zhou P, Tan GH. Cytochalasin D, a tropical fungal metabolite, inhibits CT26 tumor growth and angiogenesis. *Asian Pac J Trop Med*. 2012;5:169–174.
32. Baroncelli L, Bonaccorsi J, Milanese M, et al. Enriched experience and recovery from amblyopia in adult rats: impact of motor, social and sensory components. *Neuropharmacology*. 2012;62:2388–2397.
33. Sato I, Konishi K, Mikami A, Sato T. Developmental changes in enzyme activities and in morphology of rat cortex mitochondria. *Okajimas Folia Anat Jpn*. 2000;76:353–361.
34. Veiga FMS, Graus-Nunes F, Rachid TL, Barreto AB, Mandarim-de-Lacerda CA, Souza-Mello V. Anti-obesogenic effects of WY14643 (PPAR-alpha agonist): hepatic mitochondrial enhancement and suppressed lipogenic pathway in diet-induced obese mice. *Biochimie*. 2017;140:106–116.
35. Wen JJ, Cummins CB, Radhakrishnan RS. Burn-induced cardiac mitochondrial dysfunction via interruption of the PDE5A-cGMP-PKG pathway. *Int J Mol Sci*. 2020;21:2350.
36. He HY, Ray B, Dennis K, Quinlan EM. Experience-dependent recovery of vision following chronic deprivation amblyopia. *Nat Neurosci*. 2007;10:1134–1136.
37. Maya Vetencourt JF, Sale A, Viegi A, et al. The antidepressant fluoxetine restores plasticity in the adult visual cortex. *Science*. 2008;320:385–388.
38. Pizzorusso T, Medini P, Landi S, Baldini S, Berardi N, Maffei L. Structural and functional recovery from early monocular deprivation in adult rats. *Proc Natl Acad Sci USA*. 2006;103:8517–8522.
39. Silingardi D, Scali M, Belluomini G, Pizzorusso T. Epigenetic treatments of adult rats promote recovery from visual acuity deficits induced by long-term monocular deprivation. *Eur J Neurosci*. 2010;31:2185–2192.
40. Spolidoro M, Baroncelli L, Putignano E, Maya-Vetencourt JF, Viegi A, Maffei L. Food restriction enhances visual cortex plasticity in adulthood. *Nat Commun*. 2011;2:320.
41. Bubb MR, Spector I, Beyer BB, Fosen KM. Effects of jasplakinolide on the kinetics of actin polymerization. An explanation for certain in vivo observations. *J Biol Chem*. 2000;275:5163–5170.
42. Rex CS, Gavin CF, Rubio MD, et al. Myosin IIb regulates actin dynamics during synaptic plasticity and memory formation. *Neuron*. 2010;67:603–617.
43. Cooper JA. Effects of cytochalasin and phalloidin on actin. *J Cell Biol*. 1987;105:1473–1478.
44. Bubb MR, Senderowicz AM, Sausville EA, Duncan KL, Korn ED. Jasplakinolide, a cytotoxic natural product, induces actin polymerization and competitively inhibits the binding of phalloidin to F-actin. *J Biol Chem*. 1994;269:14869–14871.
45. Visegrady B, Lorinczy D, Hild G, Somogyi B, Nyitrai M. The effect of phalloidin and jasplakinolide on the flexibility and thermal stability of actin filaments. *FEBS Lett*. 2004;565:163–166.
46. Beaver CJ, Ji Q, Fischer QS, Daw NW. Cyclic AMP-dependent protein kinase mediates ocular dominance shifts in cat visual cortex. *Nat Neurosci*. 2001;4:159–163.
47. Di Cristo G, Berardi N, Cancedda L, et al. Requirement of ERK activation for visual cortical plasticity. *Science*. 2001;292:2337–2340.
48. Hubel DH, Wiesel TN. The period of susceptibility to the physiological effects of unilateral eye closure in kittens. *J Physiol*. 1970;206:419–436.
49. Mataga N, Imamura K, Shiomitsu T, Yoshimura Y, Fukamauchi K, Watanabe Y. Enhancement of mRNA expression of tissue-type plasminogen activator by L-threo-3,4-dihydroxyphenylserine in association with ocular dominance plasticity. *Neurosci Lett*. 1996;218:149–152.
50. Mower AF, Liao DS, Nestler EJ, Neve RL, Ramoa AS. cAMP/Ca^{2+} response element-binding protein function is essential for ocular dominance plasticity. *J Neurosci*. 2002;22:2237–2245.
51. Taha S, Hanover JL, Silva AJ, Stryker MP. Autophosphorylation of alphaCaMKII is required for ocular dominance plasticity. *Neuron*. 2002;36:483–491.
52. Fifkova E. The effect of monocular deprivation on the synaptic contacts of the visual cortex. *J Neurobiol*. 1969;1:285–294.
53. Lyckman AW, Horng S, Leamey CA, et al. Gene expression patterns in visual cortex during the critical period: synaptic stabilization and reversal by visual deprivation. *Proc Natl Acad Sci USA*. 2008;105:9409–9414.
54. Sato M, Stryker MP. Distinctive features of adult ocular dominance plasticity. *J Neurosci*. 2008;28:10278–10286.
55. Tropea D, Van Wart A, Sur M. Molecular mechanisms of experience-dependent plasticity in visual cortex. *Philos Trans R Soc Lond B Biol Sci*. 2009;364:341–355.
56. Espinosa JS, Stryker MP. Development and plasticity of the primary visual cortex. *Neuron*. 2012;75:230–249.

Investigative Ophthalmology & Visual Science